JGR Atmospheres

RESEARCH ARTICLE
10.1029/2025JD044043

Haboobs on Slopes

Nicholas M. Falk[1], Leah D. Grant[1], and Susan C. van den Heever[1]

[1]Department of Atmospheric Science, Colorado State University, Fort Collins, CO, USA

Key Points:

- As topographic slope increases, anabatic winds decrease downslope haboob propagation speeds while having little impact on upslope speeds
- As topographic slope increases, anabatic winds loft increasingly greater masses of dust, whereas haboob-related emission changes little
- Increasing surface roughness decreases haboob propagation speeds and, except on extreme slopes, reduces the total mass of dust lofted

Supporting Information:

Supporting Information may be found in the online version of this article.

Correspondence to:

N. M. Falk,
nick.falk@colostate.edu

Citation:

Falk, N. M., Grant, L. D., & van den Heever, S. C. (2025). Haboobs on slopes. *Journal of Geophysical Research: Atmospheres*, *130*, e2025JD044043. https://doi.org/10.1029/2025JD044043

Received 2 APR 2025
Accepted 16 NOV 2025

Author Contributions:

Conceptualization: Nicholas M. Falk, Leah D. Grant, Susan C. van den Heever
Data curation: Nicholas M. Falk
Formal analysis: Nicholas M. Falk, Leah D. Grant, Susan C. van den Heever
Funding acquisition: Leah D. Grant, Susan C. van den Heever
Methodology: Nicholas M. Falk
Resources: Leah D. Grant, Susan C. van den Heever
Software: Nicholas M. Falk
Supervision: Leah D. Grant, Susan C. van den Heever
Visualization: Nicholas M. Falk
Writing – original draft: Nicholas M. Falk

Abstract The impacts of topographic slope on daytime haboob propagation speeds and dust lofting are examined along with how these impacts are modulated by surface roughness length. A suite of 20 idealized, large-eddy simulations are run with varied linear topographic slopes and surface roughness lengths. It is found that on flat ground, greater surface roughness increases drag on haboobs and causes haboobs to dissipate faster, thereby decreasing both haboob propagation speeds and dust lofting. In simulations with sloped topography, upslope anabatic winds form due to solar heating. As topographic slope and surface roughness are increased, the anabatic winds become faster. Greater surface roughness causes more drag on the anabatic wind, but this is counteracted by greater sensible heat fluxes driving a stronger pressure gradient. These anabatic winds act to advect haboobs upslope. Hence, as the topographic slope is increased, downslope haboob propagation speeds are decreased, and upslope haboob propagation speeds remain mostly unchanged. Anabatic winds act to loft dust as well leading to increased dust lofting jointly by the haboob and anabatic winds as topographic slopes are increased.

Plain Language Summary Cold pools are regions of cold air that form below thunderstorms because of the evaporation of rain. In dry regions such as deserts, gusty winds from cold pools can lift dust off the ground and form sandstorms called haboobs. Haboobs often occur on sloped terrain, so the goal of this study is to understand how sloped terrain affects haboobs during the daytime. Computer simulations of haboobs are conducted to achieve this goal. Simulations which include a slope produce an upslope wind. Such upslope winds are commonly observed in the real atmosphere. This wind acts as a headwind to the haboobs, causing them to move slower down the slopes than they would normally move on flat ground. The upslope wind also lifts dust, causing a dustier sandstorm to be formed on sloped ground compared to flat ground. Rugged slopes warm up faster than smoother slopes, causing faster upslope winds and faster dissipating haboobs.

1. Introduction

Haboobs are convective cold pools, which loft mineral dust from the surface into the atmosphere (Sutton, 1925). They contribute a substantial fraction of the dust emitted from the surface. For example, 40%–50% of the emitted dust in the Sahara (Bergametti et al., 2017; Heinold et al., 2013; Marsham et al., 2013) and 30% in the southern Arabian Peninsula (Miller et al., 2008) are produced by haboobs. Understanding the processes influencing atmospheric dust loading is critical, since dust alters the atmospheric radiative balance (Slingo et al., 2006; Sokolik & Toon, 1996), serves as cloud condensation nuclei and ice nuclei (DeMott et al., 2003; Field et al., 2006; Seigel et al., 2013; Twohy et al., 2009), fertilizes the oceans and the Amazon rainforest (Babin et al., 2004; Bristow et al., 2010; Martin et al., 1990), causes motor vehicle accidents by reducing visibility (Ashley et al., 2015; Lader et al., 2016; Li et al., 2018), and contributes to respiratory disease (Griffin, 2007; Kanatani et al., 2010; Tong et al., 2023). Current emissions of dust are greater than preindustrial dust emissions, and these emissions may continue to increase due to climate change, land use change, and other anthropogenic activities (Ginoux et al., 2012; Mahowald et al., 2010; Munson et al., 2011; Neff et al., 2008). Despite its importance, dust emission is not well represented in weather and climate models (Ansmann et al., 2017; Knippertz & Todd, 2012; Kok et al., 2023; Wu et al., 2020), and the difficulties of accurately representing haboobs in such models may be a large source of error (Bukowski & van den Heever, 2020; Pantillon et al., 2015, 2016; Saleeby et al., 2019; Walker et al., 2009).

Topography can impact haboobs and associated dust lofting. Haboobs—and dust emissions in general—often occur in regions of complex topography such as northern Africa, the Arabian Peninsula, and the southwest United States (Adams & Comrie, 1997; Knippertz et al., 2007; Miller et al., 2008; Tanaka & Chiba, 2006). The mountain-plains circulation in the Sahara, driven by the Atlas and Hoggar mountains, is similar to Alpine-pumping (Flamant et al., 2007; Lugauer et al., 2003). This pumping can initiate convection over high terrain,

Writing – review & editing: Nicholas M. Falk, Leah D. Grant, Susan C. van den Heever

leading to the formation of haboobs, which then accelerate downslope (Emmel et al., 2010; Knippertz et al., 2007). The Saharan mountain-plains circulation can also redirect dust lofted by haboobs toward Iberia and lead to further dust lofting (Dhital et al., 2022). Downslope windstorms have been shown to loft dust in North Africa and the Arabian Peninsula (Pokharel et al., 2017). Heinold et al. (2013) investigated drivers of dust emission in summertime West Africa. They speculated that topographically driven circulations could contribute to unknown sources of dust emission, which make up ∼20% of total emissions.

Topographic effects on cold pools have been investigated using mostly observational data or case study simulations. Cold pools in Arizona, New Mexico, and Colorado have been shown to propagate more quickly downhill than uphill or over complex terrain (Luchetti, Friedrich, & Rodell, 2020; Luchetti, Friedrich, Rodell, et al., 2020). The ambient wind appears to influence the propagation speed of uphill propagating cold pools but not cold pools propagating downhill or over complex terrain (Luchetti, Friedrich, & Rodell, 2020; Luchetti, Friedrich, Rodell, et al., 2020). Simulations have also shown that the terrain can slow (H. Liu et al., 2022) or even block (Mulholland et al., 2019) cold pools. Johnson et al. (2014) simulated a cold pool over the Colorado Rocky Mountains and noted hydraulic jumps on the lee side of ridgelines. Compared to a flat surface, laboratory tank density currents propagate faster downslope (Dai & Huang, 2016; Dai et al., 2012; He et al., 2017) and density currents moving upslope become vertically thinner and move slower (De Falco et al., 2020; Lombardi et al., 2015; Marleau et al., 2014; Simpson, 1997).

A number of other factors known to affect haboob propagation and dust lofting may be important in modulating the impact of topographic slopes on haboobs. Huang et al. (2018) (hereafter H18) tested the impact of grid spacing and prescribed surface sensible heat fluxes in idealized simulations of haboobs. They found that finer grid spacing led to greater turbulent mixing, and hence haboobs, which dissipated faster and propagated slower (as shown by earlier studies such as Straka et al. (1993) and Grant and van den Heever (2016)) as well as lofted less dust. Greater sensible heat fluxes similarly led to faster dissipating and slower haboobs consistent with the prior results of Grant and van den Heever (2016, 2018) but also greater dust lofting due to increased downward momentum transport.

Bukowski and van den Heever (2021) (hereafter BvdH21) investigated the radiative effects of dust in case study simulations of haboobs. Scattering of shortwave radiation during the day caused colder, more intense, dustier haboobs, whereas the absorption of longwave radiation at night caused warmer, weaker haboobs. However, the stable nocturnal surface layer caused increased haboob propagation speeds consistent with previous theoretical investigations of the impacts of stable layers on density currents (C. Liu & Moncrieff, 2000; Seigel & van den Heever, 2012b) as well as larger dust emission at night. Diurnal variations in haboob propagation speeds over the Sahara have also been observed (Caton Harrison et al., 2021) in support of these modeling studies. Bukowski and van den Heever (2022) (hereafter BvdH22) examined the influence of time of day, initial haboob temperature, vegetation type, soil type, and soil moisture on haboobs and associated dust lofting. They found the most important of these factors were the initial haboob temperature and vegetation type. Colder initial temperatures drove faster propagation, faster wind speeds, and hence more dust lofting. Vegetation with greater roughness lengths decreased dust emission but also increased sensible and latent heat fluxes. BvdH22 found that interpreting the effect of vegetation type was complicated because several factors—including roughness, albedo, and evapotranspiration—are all dependent on vegetation type. Finally, the erodible surface fraction can also influence dust emissions (Saleeby et al., 2019; Walker et al., 2009), thereby potentially impacting haboob propagation via radiative effects.

The aforementioned research on haboobs has covered a wide variety of topics. However, the impacts of topography on haboobs—and cold pools more generally—are still not well understood. Although observational studies and case study simulations are very valuable, idealized and/or theoretical studies are needed to draw more generalized conclusions about haboob processes. However, such idealized studies of haboobs have been very limited to date with H18 and BvdH22 being the exceptions.

The objective of this study is to investigate the impact of topographic slope on daytime haboob propagation and dust lofting along with how this impact is modulated by aerodynamic surface roughness. As BvdH22 found the largest impact on haboobs from varying vegetation type was due to roughness effects, testing roughness in isolation allows for a clearer understanding of its specific impacts. To achieve our objective, we run a suite of 20 idealized haboob simulations where two factors—topographic slope and surface roughness—are independently and simultaneously varied. In contrast to many previous studies, which have used observational data or case study

Table 1
Summary of RAMS Settings Common to All Simulations

Model setting	Value/type
Starting time	1984-08-09 2030 Z (1330 LT)
nx, ny, nz	800, 1,600, 200
dx, dy, dz	100, 100, 50 m
dt	0.5 s
Rayleigh layer depth	6 points
Rayleigh layer timescale	60 s
Coriolis force	None
Central latitude and longitude	32.3 N, 111.0 W
Data output frequency	1 min
Lateral boundary condition	Cyclic
Subgrid Turbulence Parameterization	Smagorinsky (1963) with modifications from Lilly (1962) and Hill (1974)
Radiation Parameterization	Harrington (1997)
Surface parameterization	LEAF-3 (Walko et al., 2000)
Vegetation Type	Desert, bare soil
Soil Type	Silty clay loam
Number of soil layers	11
Soil depth	0.5 m
Initial soil surface temperature offset from lowest atmospheric level	−2 K
Soil moisture	None
Aerosol Species	Dust only
Initial Bubble Horizontal Radius	6,000 m
Initial Bubble Vertical Radius	4,000 m

simulations, this suite of idealized simulations allows for the impacts of the two factors to be more clearly disentangled from each other and provides more generalized conclusions about haboob processes. A unique algorithm is developed to track the boundaries of haboobs and hence propagation speeds. The simulations are analyzed to understand how and why the two factors impact haboob propagation and dust lofting. Our findings shed new light on fundamental haboob processes and have implications for the representation of haboobs and associated dust lofting in forecast and climate models.

2. Methods

2.1. Model Setup

The suite of idealized, high-resolution simulations is run using the Regional Atmospheric Modeling System (RAMS) version 6.3.02 (Cotton et al., 2003; Pielke et al., 1992; Saleeby & van den Heever, 2013; van den Heever et al., 2022). The objective of this study is not to simulate haboobs in a specific region but rather examine haboob processes in conditions representative of typical haboob environments. In mountainous regions, scattered convective storms tend to initiate over high terrain in the afternoon and then grow upscale into the evening and overnight hours as they propagate away from the terrain (Houze, 2012). The simulations in this study are representative of haboobs from scattered afternoon convection and not organized nocturnal convection. Haboobs are introduced in simulations at 1500 LT consistent with observations of afternoon haboobs by Emmel et al. (2010) and Caton Harrison et al. (2021). To simplify the analysis, simulations are run without moisture or microphysics. The model setup conditions common to all simulations are summarized in Table 1. The topography varies only in the meridional direction. The southern half of the domain slopes linearly upward to a peak in the meridional center. The topography in the northern half of the domain is then a mirror image of the southern half, sloping downward toward the northern boundary (Figure 1a). This idealized setup allows for the basic effects of topography to be studied but prevents more complicated interactions, such as the channeling of currents in

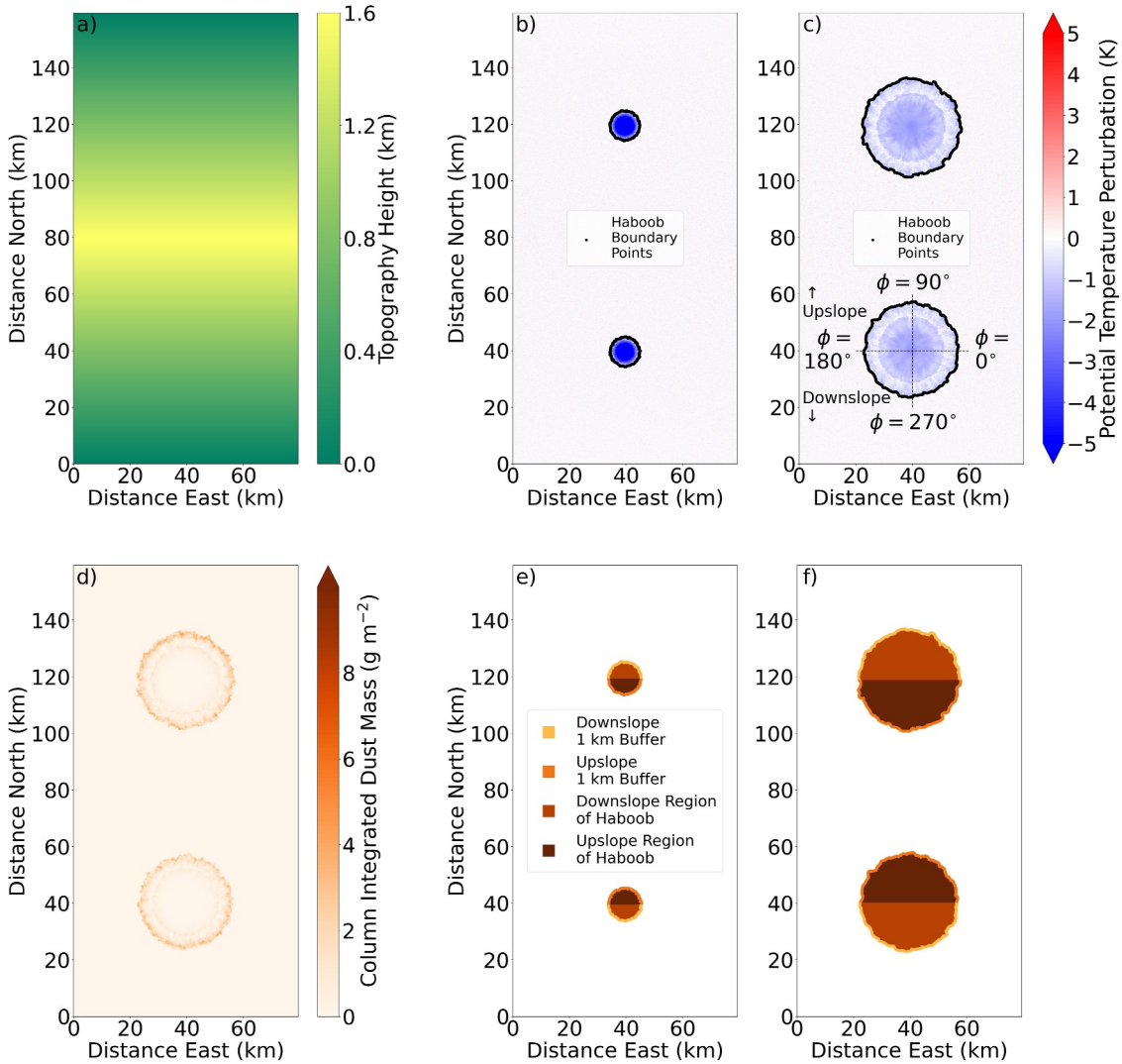

Figure 1. Model domain, topography setup, and output. All data in this figure are plotted for the SLOPE-2_ROUGH-034 simulation. Shown are (a) model topography (m); (b) 25 m AGL potential temperature perturbation (K) and haboob boundary points at 1 min; (c) as in (b) but at 30 min; (d) column integrated dust mass (g m^{-2}) at 30 min; (e) identified haboob regions at 1 min; and (f) as in (e) but at 30 min. Also indicated in (c) are the angles (ϕ) used in the haboob tracking algorithm.

valleys. The topographic slopes tested are discussed further in Section 2.3. A terrain-following sigma coordinate is used, so the vertical grid spacing varies between 29 and 50 m based both on the height of the topography and the height above ground level. The radiation parameterization assumes a flat surface, so the southern and northern halves of the domain receive nearly identical amounts of solar radiation at the surface. Only the central latitude, central longitude, and simulation starting time affect the parameterized radiation (Harrington, 1997; Stokowski, 2005), and the settings for these parameters are chosen to be representative of daytime haboobs occurring in the southwestern United States (Adams & Comrie, 1997). The dust in all simulations is radiatively inert. Simulations with radiatively active dust showed only negligible differences when compared to simulations with radiatively inert dust (not shown) contrary to the results of BvdH21. These differences are most likely the result of the shorter haboob lifetimes in this study compared to BvdH21.

The Land-Ecosystem-Atmosphere-Feedback version 3 (LEAF-3) (Walko et al., 2000) model coupled to RAMS is used to simulate an interactive land surface. All simulations apply a horizontally homogenous bare soil desert with silty clay loam soil (59% clay). These conditions were chosen because they are generally representative of environments in which haboobs form and were also tested by BvdH22. No vegetation is included, and the soil is completely dry. As has been previously demonstrated, including vegetation and/or soil moisture would lead to a

smaller mass of lofted dust (BvdH22). For more information on the impact of surface properties on dust lofting in RAMS, see BvdH22.

Simulations consist of an initial spin-up phase during which a turbulent boundary layer is allowed to develop and a subsequent analysis phase during which haboobs are initiated by releasing cold bubbles, which create a distinct and trackable boundary, following the approach of BvdH22 as well as numerous previous idealized studies of cold pools (Bryan & Rotunno, 2014a, 2014b; Grant & van den Heever, 2016; Meyer & Haerter, 2020; Seigel & van den Heever, 2012b). Simulations are initialized using a horizontally homogeneous atmospheric sounding with zero winds and a constant Brunt-Väisälä frequency of 0.005 s^{-1}. These weak statically stable conditions are used to prevent the turbulent boundary layer from growing unphysically deep. At sea level, the initial sounding has a surface temperature of 28.4°C (based on the 0Z Tucson sounding from 1984-08-10) and a surface pressure of 1,000 hPa. These values were chosen to be consistent with the time and location (southwestern United States) specified for the radiation parameterization. Density current propagation is more strongly modulated by the temperature difference between the current and its surroundings than the temperature of the current or surroundings in isolation (Benjamin, 1968). Thus, although we chose conditions based on the southwestern United States, choosing conditions based on a different region (e.g., the Sahara or the Arabian Peninsula) would likely lead to similar results. Radiative tendencies are updated every 10 min in the spin-up phase and every 1 min in the analysis phase.

At the start of the spin-up phase, random potential temperature perturbations of amplitude 0.1 K are added to the lowest 500 m of the domain to break symmetry arising from the homogeneous atmosphere. Simulations are integrated for 90 min during the spin-up phase. After the spin-up phase is completed, the simulations are restarted with a dome-like cold bubble added to both the southern and northern halves of the domain. Each of these two cold bubbles is centered in its respective domain half (Figures 1a and 1b) and is placed at the surface to facilitate tracking of the haboob boundary. Simulations are then integrated for another 90 min during the analysis phase after which the haboobs have almost entirely dissipated. All of the figures below show data from the analysis phase, and all times discussed in this paper are relative to the start of the cold bubble introduction and hence the start of the analysis phase.

2.2. Dust Emission

Dust mass flux from the surface (F_p) in RAMS is parameterized (Saleeby & van den Heever, 2013; Seigel & van den Heever, 2012a; Smith, 2007) based on the GOCART scheme (Ginoux et al., 2001), where:

$$F_p = \begin{cases} E_{z0} C s_p u_h^2 (u_h - u^*_{t,\mathrm{wet}}), & u_h > u^*_{t,\mathrm{wet}} \\ 0, & u_h \le u^*_{t,\mathrm{wet}} \end{cases}. \quad (1)$$

In Equation 1, E_{z0} is the erodible surface fraction, $u^*_{t,\mathrm{wet}}$ is the threshold friction velocity, while C, and s_p are scaling factors. Given our model setup, $E_{z0}, u^*_{t,\mathrm{wet}}, C$, and s_p are all constants. The only variable in Equation 1 is the 10 m wind speed u_h, which is calculated by assuming a logarithmic wind profile from the wind speed at the lowest model level. Dry deposition of dust is enabled. The dust-erodible fraction of every grid cell is set to 1.0. Using a spatially uniform erodible fraction facilitates a clearer analysis of idealized simulations compared to using a case-study specific erodible fraction data set. Selecting a specific erodible fraction would be highly subjective for a suite of idealized simulations. Additionally, our analysis of dust lofting focuses on proportional differences between simulations rather than focusing on the absolute masses of dust lofted, so the specific selection of the erodible fraction is not overly impactful. An erodible fraction of 1.0 can be considered an upper-bound on dust emissions (Saleeby et al., 2019). Dust emissions are also more common in low-lying areas than on sloped terrain (Prospero et al., 2002). Hence, using a realistic erodible fraction data set could lead to less dust lofting but would complicate analysis. Readers interested in further details of the dust scheme in RAMS are referred to Saleeby and van den Heever (2013) and Seigel and van den Heever (2012a).

The effect of low-level winds on dust lofting is evident in Figure 1, which shows the output from an example simulation. Most of the dust mass is at the leading edges of the haboobs (Figures 1c and 1d), where the fastest wind speeds and largest convergence are located (not shown).

2.3. Sensitivity Experiments

All combinations of five topographic slopes and four surface roughness lengths are tested giving a total of 20 simulations. The five different topographic slopes are grades of 0% (flat ground), 1%, 2%, 3%, and 5% (hereafter named SLOPE-0, SLOPE-1, SLOPE-2, SLOPE-3, and SLOPE-5 respectively). For example, Figure 1a shows topography with a grade of 2% (SLOPE-2) where the terrain rises 1.6 km over a horizonal distance of 80 km. These grades were chosen based on analysis of topography in the southwestern United States, northern Africa, and the Arabian Peninsula (see Text S1 in Supporting Information S1 for specific examples).

As discussed previously, two cold bubbles are initially centered on the northern and southern halves of the domain in each simulation. In our analysis, the northern and southern domain halves are treated independently of each other. All southern cold bubbles have initial minimum potential temperature perturbations of −10 K based on BvdH22. For the northern cold bubbles, the temperature perturbations are scaled such that the latent cooling required to produce them is the same as to produce a −10 K cold bubble on flat ground at sea level. Since the air density is less at higher elevations, but the latent cooling required to produce the initial bubbles is held constant, the northern cold bubbles become slightly colder as the topographic slope increases. The northern cold bubbles are included to test this effect of reduced air density on latent cooling at higher altitudes. Apart from propagating slightly faster and lofting a little more dust than their southern counterparts due to being slightly colder, the northern haboobs produce broadly similar results to the southern haboobs and hence are not shown in this manuscript, other than in Figures 1 and 2.

The four soil surface roughness lengths tested are 0.001, 0.034, 0.066, and 0.100 m (hereafter named ROUGH-001, ROUGH-034, ROUGH-066, ROUGH-100, respectively). These correspond to the roughness lengths of the four different vegetation types tested in BvdH22 (desert, short grassland, semidesert, and crop-grassland respectively). Greater roughness will lead to a larger downward transport of momentum at the surface in turn causing greater sensible and latent heat fluxes (BvdH22). The simulations are named using their topographic slope and surface roughness length. For example, the SLOPE-2_ROUGH-034 simulation shown in Figure 1 has a 2% topographic slope and a 0.034 m surface roughness length.

2.4. Analysis Approach

An algorithm was developed to track the boundaries of the haboobs in time in polar coordinates, thereby objectively determining propagation speeds. The algorithm is described in detail in Text S2 of the Supporting Information S1. For a given time t and angle ϕ, the algorithm yields a haboob boundary point $\boldsymbol{b}$, which is an (x, y) coordinate pair. Note $\phi = 0$ points east and ϕ increases moving counterclockwise around haboobs (Figure 1c). Haboob boundary points are shown for the example haboobs demonstrated in Figures 1b and 1c. Propagation speeds are calculated as a function of time, and the mean is taken over all haboob boundary points for each haboob, the results of which are shown in Figure 2a. Haboobs accelerate for the first ∼10 min after initialization and begin to decelerate thereafter. Figure 2b demonstrates the percentage of lost haboob boundary points, which occur due to the algorithm mistakenly identifying boundary layer turbulence as the haboob boundary and that must be recovered by radial interpolation (see Text S2 in Supporting Information S1 for more information). Haboob boundaries are not tracked after 30 min, as the number of lost haboob boundary points increases substantially after ∼25 min due to the warming of the simulated haboobs. This does not mean that all haboobs completely dissipate in 30 min, merely that the tracking algorithm becomes unreliable after this time. Haboobs with lifetimes between 30 and 90 min have been documented (Caton Harrison et al., 2021). The relatively short lifetimes of haboobs in this study are typical of cold pools originating from scattered convection (Drager et al., 2020). In all subsequent figures, haboob propagation speeds $v(\phi)$ are always calculated by taking the mean propagation speed between 10 and 30 min:

$$v(\phi) = \frac{\|\boldsymbol{b}(30\ \text{min}, \phi) - \boldsymbol{b}(10\ \text{min}, \phi)\|}{20\ \text{min}}. \tag{2}$$

Thus, $v(\phi)$ represents the mean propagation speed of haboobs after their initial acceleration but before they dissipate to the point of becoming difficult to identify and track. Results are not qualitatively sensitive to the starting time chosen for $v(\phi)$.

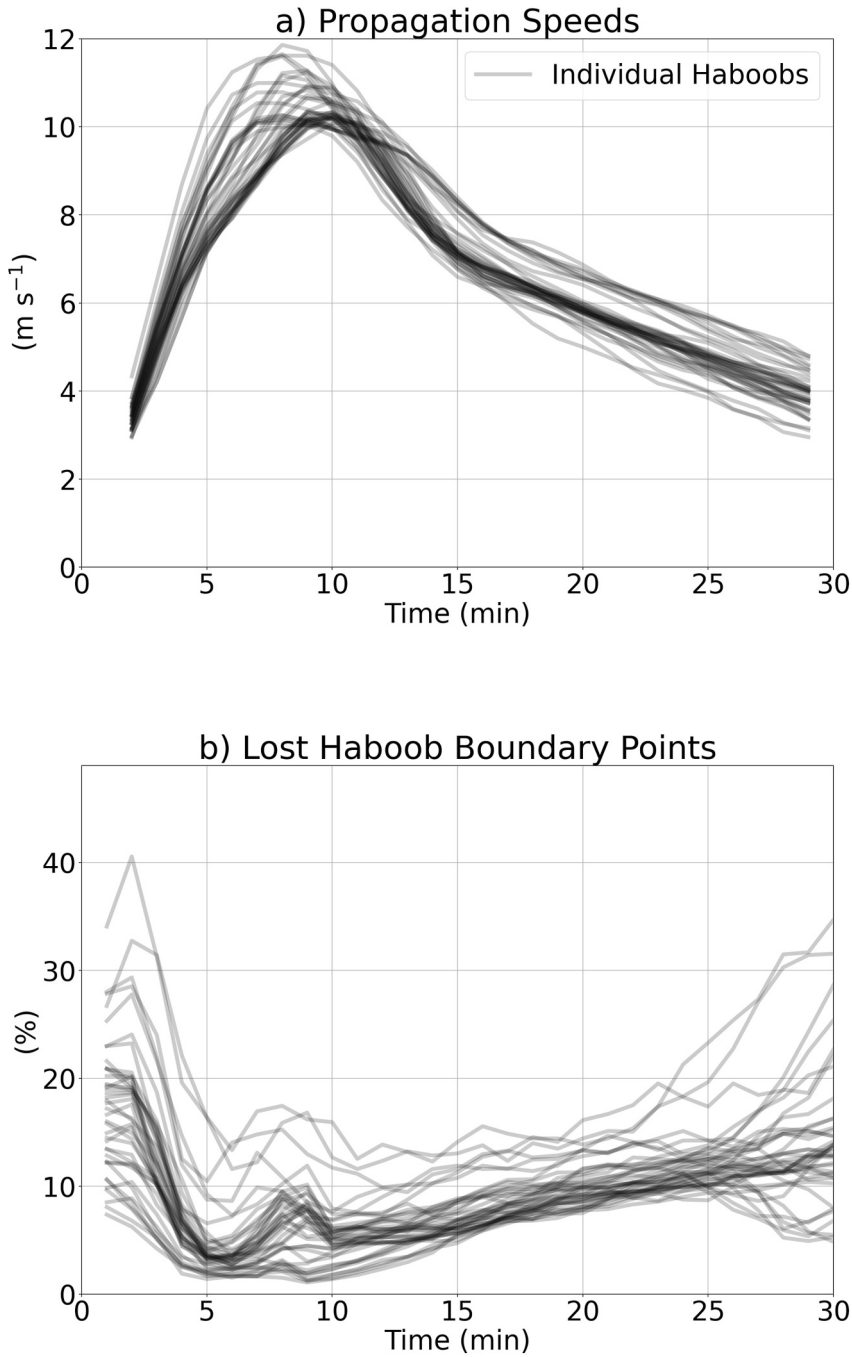

Figure 2. Haboobs begin to decelerate after ~10 min and become difficult to track ~30 min. (a) Time series of propagation speeds for all the haboobs captured in the idealized simulations. (b) Percentage of lost haboob boundary points for all the haboobs as a function of time.

Identifying the haboob boundary points allows for the identification of model gridpoints located within specific regions of haboobs. Figures 1e and 1f show how each haboob can be subdivided into a downslope region and an upslope region. These two regions can also be considered together to yield all model grid-points falling within a haboob. The internal haboob regions are determined for every haboob at every output time between 1 and 30 min (i.e., when haboob boundary points can be identified).

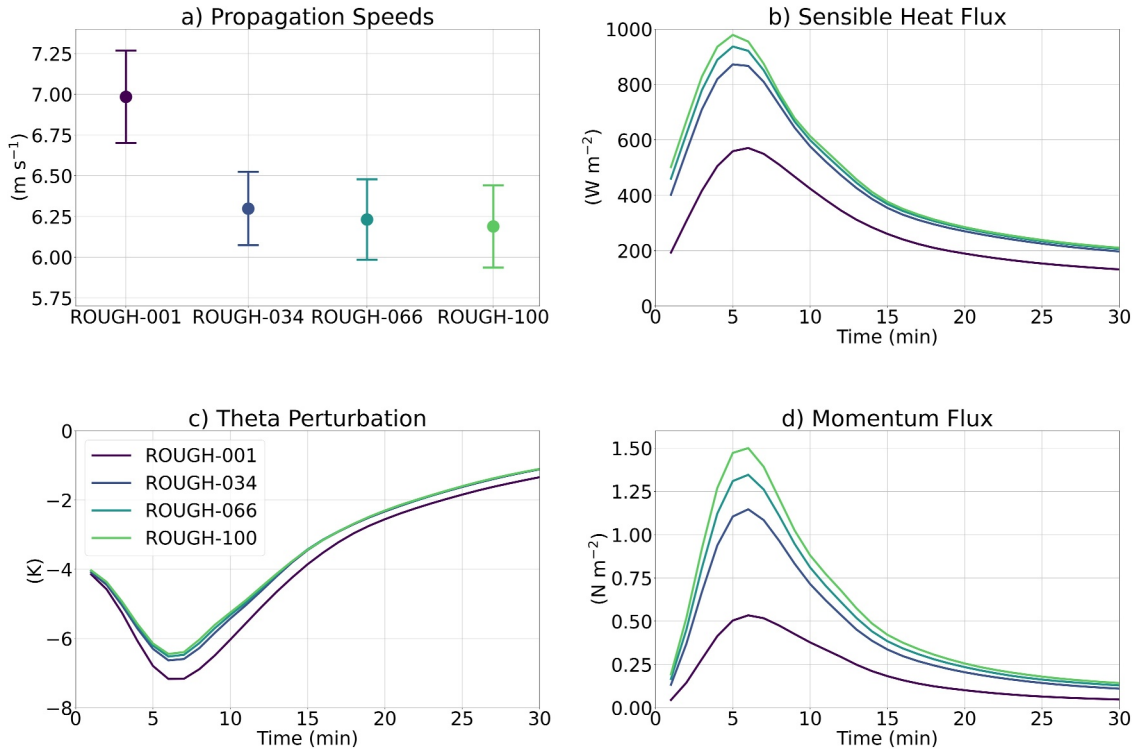

Figure 3. Haboobs on flat terrain are slowed by increasing surface roughness. All data in this figure are from SLOPE-0 simulations. (a) Haboob propagation speeds as a function of surface roughness. In (a) circles (error bars) represent mean (standard deviation) propagation speeds over all haboob boundary points. (b) Time series of in-haboob mean surface sensible heat flux for different surface roughness (line colors). (c) as in (b) but for the 25 m AGL potential temperature perturbation (defined in Text S2 in Supporting Information S1). (d) as in (b) but for the horizontal momentum flux.

3. Results

3.1. Haboobs on Flat Terrain

We first investigate how the daytime haboobs in our simulations are impacted by surface roughness on flat terrain before considering their behavior on sloped terrain. Figure 3a demonstrates the mean and standard deviation propagation speeds for haboobs on flat terrain. The mean and standard deviation are taken over all angles $\boldsymbol{\phi}$ (i.e., radially around the entire haboob), since haboobs on featureless terrain without background winds should expand equally in all directions at about the same rate. Increasing surface roughness from 0.001 to 0.034 m slows the haboobs' propagation speeds by ∼0.75 m s^{-1} (∼10%), but subsequent increases in surface roughness produce smaller decreases in propagation speeds (Figure 3a). Density current propagation speeds are directly tied to temperature perturbations (Benjamin, 1968), so haboobs which dissipate more rapidly through warming should propagate more slowly than those which dissipate less rapidly. Increased surface roughness enhances the sensible heat fluxes within the haboobs which, in turn, increases the in-haboob warming (Figure 3b). So, larger surface roughness causes haboobs to dissipate faster—and thus propagate slower—than smaller surface roughness (Figure 3c). Additionally, increased surface roughness leads to greater surface drag on the haboobs, thereby further reducing propagation speeds (Figure 3d). Several previous studies have similarly shown increased surface roughness and/or sensible heat fluxes leading to faster dissipation of cold pools on flat terrain (Bukowski & van den Heever, 2022; Gentine et al., 2016; Grant & van den Heever, 2016, 2018; Huang et al., 2018).

We now investigate the dust lofted by the passage of haboobs on flat terrain. Total dust mass initially increases rapidly with time and then asymptotes between 30 and 90 min for haboobs on flat ground (Figure 4a). This behavior suggests that dust lofting mostly ceases once haboobs have dissipated after ∼30 min, and that the dry deposition of dust over the remaining time period is minimal. H18 also argued that the deposition of dust should be minimal in haboob simulations lasting <6 hr, as vertical wind speeds in turbulent daytime haboobs are greater than dust particle fall speeds, thereby preventing dust particles from settling to the surface. Recall in these simulations that dust emission from the surface only varies due to changes in low-level wind speed and is not a

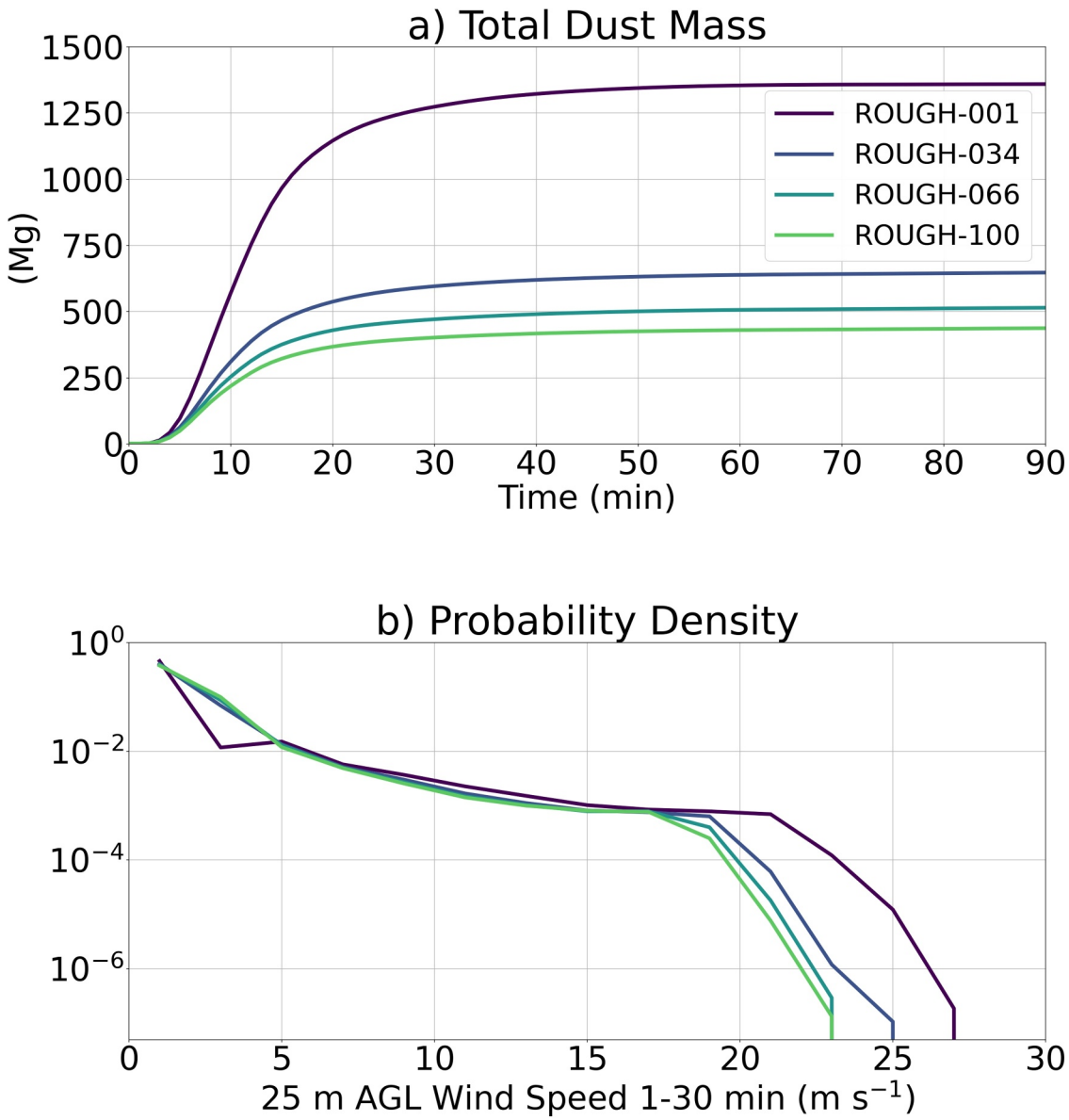

Figure 4. For haboobs on flat terrain, increased surface roughness decreases the total dust mass by decreasing wind speeds. (a) Time series of total dust mass for SLOPE-0 simulations, where surface roughness is indicated by line color. (b) Probability density function of 25 m AGL wind speed in SLOPE-0 simulations.

function of surface type, erodible surface fraction, and soil moisture. Wind speeds at 25 m above ground level (AGL) decrease with increasing surface roughness (Figure 4b). It follows that increased roughness decreases the total mass of dust lofted (Figure 4a). The total dust mass is more than halved between ROUGH-001 and ROUGH-100 in the SLOPE-0 simulations (Figure 4a). Taken together, Figures 3 and 4 show that increased surface roughness alone can decrease haboob dust lofting via faster haboob dissipation and increased surface drag. Note that if the erodible surface fraction was allowed to vary with surface roughness, then the impact of roughness would likely be even more pronounced.

BvdH22 and H18 both evaluated dust lofting, surface roughness, and/or sensible heat flux. In a few tests where they neglected the erodible surface fraction, BvdH22 argued, as we do here that colder and slower-dissipating haboobs should loft more dust because of the faster, longer-lived near-surface winds produced in association with stronger, longer-duration cold pools. However, our result—that on flat terrain increased surface roughness decreases haboob dust lofting—is somewhat at odds with H18. They found that as the sensible heat flux is increased, downward mixing of momentum toward the surface is increased, leading to stronger low-level wind

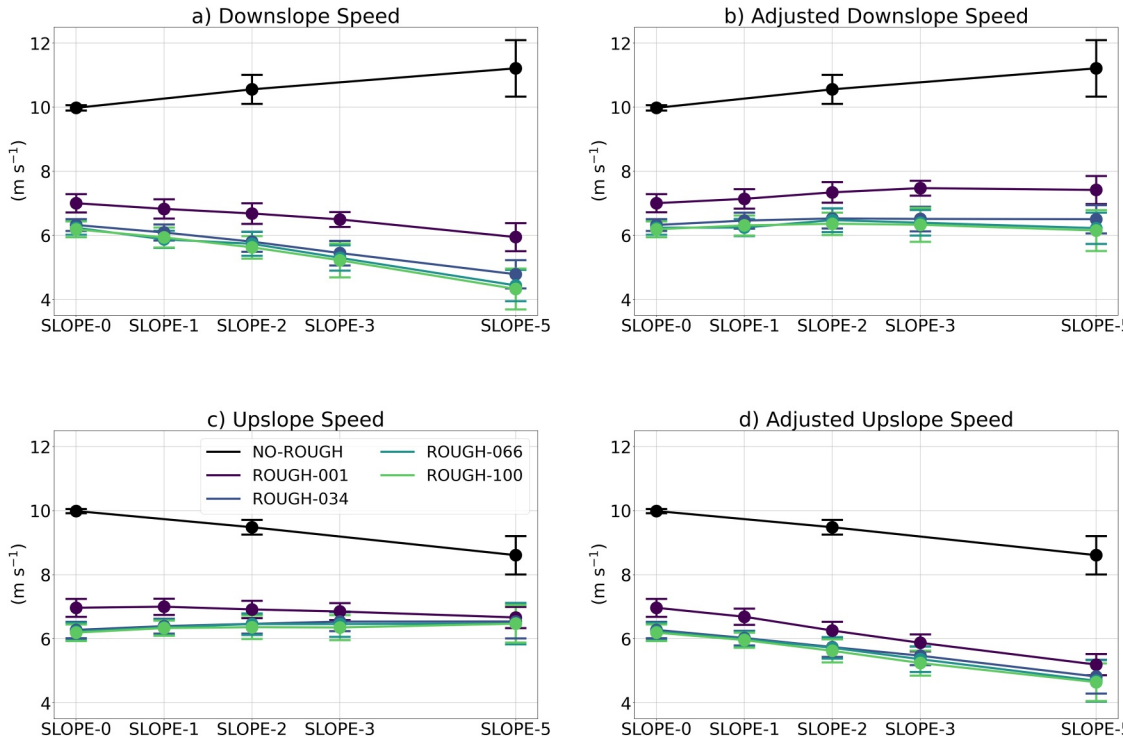

Figure 5. As the topographic slope increases, anabatic winds cause downslope haboob propagation speeds to decrease and upslope speeds to be mostly unchanged. (a) Downslope haboob propagation speeds as a function of topographic slope for different surface roughness (line colors) including NO-ROUGH simulations with no spin-up, no parameterized radiation, and a free-slip surface (black). In (a) circles (error bars) represent mean (standard deviation) propagation speeds. (b) as in (a) but with propagation speeds adjusted for anabatic wind speed. (c, d) as in (a, b) but for upslope propagation speeds.

speeds and greater dust lofting rates. There are several possible explanations for the discrepancy between H18's results and our results. First, we vary surface roughness length while H18 varied sensible heat flux. As such, H18 did not consider the effects of increased drag on haboob dust lofting. Second, H18 prescribed constant sensible heat fluxes, whereas the sensible heat fluxes in this study are determined using a bulk formula. Grant and van den Heever (2016, 2018) demonstrated that prescribed and interactive sensible heat flux formulations have significantly different effects on cold pool properties and processes. Third, we simulate the entire lifetime of haboobs while H18 did not. H18 speculated that, if they ran their simulations longer, increased sensible heat flux may lead to decreased haboob lifetimes and thus decreased dust lofting. Finally, our simulations are all three-dimensional while all but one of H18's simulations were two-dimensional, so differences in the representation of turbulence in 3D and 2D likely play a role as well. We now proceed to investigate the effects of topographic slope on haboobs.

3.2. Haboobs on Sloped Terrain

As shown in prior studies and discussed above, haboobs are expected to propagate at different speeds when traveling upslope compared to downslope. Hence, upslope and downslope propagation speeds are computed separately for all of the haboobs in this analysis. Figure 5a shows mean and standard deviation propagation speeds, $\boldsymbol{v}(\boldsymbol{\phi})$, where the mean and standard deviation are taken for angles between 180° and 0°, that is, the downslope sides of haboobs (Figure 1c). Figure 5c analogously shows mean and standard deviation propagation speeds for the upslope sides of haboobs (i.e., for angles between 0° and 180°). Note that propagation speeds shown in Figure 5 fall within the range of haboob and cold pool propagation speeds reported in prior literature (see Figure 8a from Caton Harrison et al. (2021) along with Table 1 and Figure 3 from Falk, Grant, van den Heever, et al. (2025)). It is evident that as the topographic slope increases, downslope haboob propagation speeds decrease while upslope speeds are mostly unchanged (Figures 5a–5c). This is contrary to previous literature, which has found that cold pools and laboratory tank density currents propagate faster downslope and slower upslope (Dai et al., 2012; Luchetti, Friedrich, & Rodell, 2020; Luchetti, Friedrich, Rodell, et al., 2020; Marleau et al., 2014). The differences in our results are due to the presence of an anabatic wind.

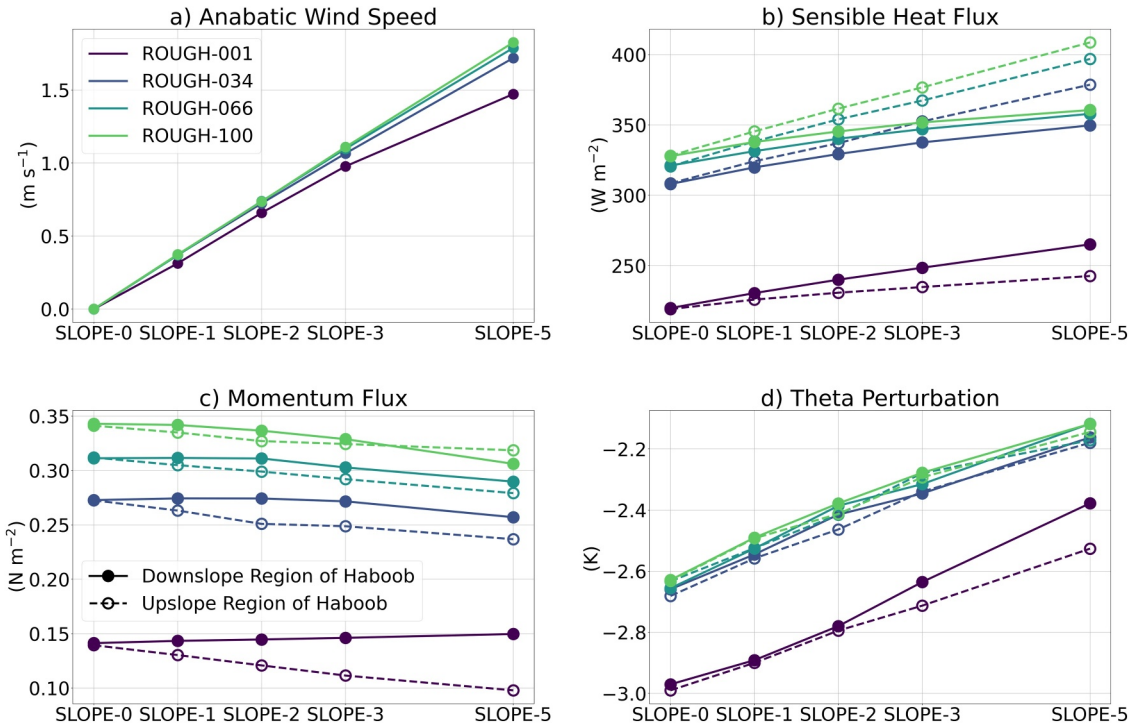

Figure 6. Increasing topographic slope and surface roughness lead to increased anabatic wind speeds, in-haboob surface sensible heat fluxes, and haboob dissipation. (a) Mean 25 m AGL meridional wind speed at the time cold bubbles are initiated as a function of topographic slope for different surface roughness (line colors). (b) Mean sensible heat flux between 10 and 30 min for the downslope (solid circles and lines) and upslope (hollow circles and dashed lines) regions of haboobs as a function of slope for different roughness (line colors). (c) as in (b) but for horizontal momentum flux. (d) as in (b) but for 25 m AGL potential temperature perturbation.

The anabatic wind forms during the spin-up phase of our simulations (see Figure S1 in Supporting Information S1 for examples). The development of anabatic winds in response to the daytime heating of topographic slopes is frequently observed and is consistent with mountain valley circulation theories (Defant, 1951; Farina & Zardi, 2023). Figure 6a demonstrates the speed of the anabatic wind by showing the mean low-level meridional wind at the time the initial cold bubbles are added. Recall that the radiation parameterization does not consider the topographic slope, so the downwelling shortwave radiation at the surface is similar across the domains of all simulations during the spin-up phase. Thus, although the anabatic winds form because of the heating of the sloped surfaces, they are not due to slope-induced differential heating but rather form because the heating creates a pressure gradient between the sloped surface and the ambient environment (not shown). The latter process is also important in observed anabatic wind formation.

The anabatic wind speed increases as topographic slope is increased (Figure 6a). For steeper topographic slopes, air is warmed over a deeper layer (i.e., the height of the topography) thereby driving a larger pressure gradient force between the sloped surface and the ambient environment compared to gentler slopes. Greater roughness lengths drive larger sensible heat fluxes, thereby increasing the heating rates of near-surface air, and subsequently causing larger pressure gradient forces compared to lower roughness lengths (not shown). Greater roughness lengths also increase the drag on the anabatic wind. The experiments show that the anabatic wind speed weakly increases as the surface roughness is increased (Figure 6a), indicating that the effect of increased sensible heat fluxes outweighs the effect of increased drag. Finally, there is a positive feedback to anabatic wind speeds detailed as follows: as anabatic wind speeds increase, these greater wind speeds drive larger sensible heat fluxes, which in turn increase heating, causing an even faster anabatic wind speed (Kirshbaum, 2013).

Figure 5b (5d) shows the downslope (upslope) haboob propagation speeds relative to the anabatic wind speeds, that is, the anabatic wind speeds have been added (subtracted) from the propagation speeds shown in Figure 5a (5c). When adjusting for advection due to the anabatic winds, it is evident that as the topographic slopes become steeper, downslope haboob propagation speeds are mostly unchanged while upslope haboob propagation speeds decrease. The anabatic wind speed at 25 m AGL and 0 min is used when making this adjustment, but the results

shown in Figures 5b and 5d are not overly sensitive to the time or depth chosen. After taking into account the anabatic wind velocities, the behavior of the haboob propagation speeds is more consistent with findings of past research (Dai et al., 2012; Luchetti, Friedrich, & Rodell, 2020; Luchetti, Friedrich, Rodell, et al., 2020; Marleau et al., 2014). Although previous studies have disagreed about the influence of ambient winds on cold pool propagation speeds (Luchetti, Friedrich, & Rodell, 2020; Luchetti, Friedrich, Rodell, et al., 2020), the ambient anabatic wind plays an important role in altering the propagation speeds in this study.

Even after accounting for the anabatic wind speeds, downslope haboob propagation speeds do not seem to meaningfully increase on steeper slopes (Figure 5b). To ensure that this relationship is not a result of shortfalls in our simulation setup or analysis, three simplified simulations (hereafter called NO-ROUGH) were conducted with no spin-up, the radiation parameterization turned entirely off, and a free-slip surface. We find that no anabatic wind forms due to the lack of sensible heat fluxes in the NO-ROUGH simulations. Furthermore, the haboobs are observed to propagate progressively faster downslope and slower upslope with increasing slope than they do on flat terrain in these simplified simulations (Figure 5). Our model setup produces results that are therefore consistent with traditional density current theory. The NO-ROUGH simulations also show that a mechanism beyond the anabatic wind is slowing the downslope propagation of haboobs in our suite of sensitivity simulations. As the topographic slope increases, sensible heat flux in both the upslope and downslope regions of haboobs increases likely because of the anabatic winds driving faster low-level wind speeds (Figure 6b). Hence, as the haboobs are warmed, the temperature perturbations between the haboobs and their environment decreases, and the haboobs slow down (Figure 6d). This more rapid dissipation of haboobs on increasingly sloped terrain explains why there is not a clear increase in downslope propagation speeds when adjusting for the anabatic wind speed (Figure 5b).

Topographic slope also has a marked impact on dust emissions. After 30 min, the mass of dust lofted inside the haboobs and the total mass of lofted dust are nearly identical for SLOPE-0 simulations (Figure 7a), which is expected because the SLOPE-0 simulations do not produce anabatic winds nor dust lofting outside of the haboobs. However, as topographic slope increases, the total dust mass is increasingly greater than the in-haboob dust mass due to dust lofting by anabatic winds (Figure 7a). See Text S3 in Supporting Information S1 for a description of how the mass of dust lofted by haboobs and by anabatic winds is determined in Figure 7.

After 90 min, the time by which the haboobs have essentially dissipated, the increase in dust lofting due to increasingly sloped terrain is more pronounced than at 30 min. There is approximately 1.5–4.5 times more dust mass in the SLOPE-5 simulations than the SLOPE-0 simulations depending on the surface roughness (Figure 7b). Most of the difference in total dust mass between 90 min (Figure 7b) and 30 min (Figure 7a) is due to lofting by the anabatic wind. For the SLOPE-5 simulations, the effect of the anabatic wind is so pronounced that the total dust mass is about the same for all roughnesses (Figure 7b). Hence, as surface roughness is increased on the most extreme topographic slope, enhanced dust lofting from the larger anabatic wind speed counteracts decreases in dust lofting from faster haboob dissipation and larger drag. Recall that as surface roughness increases, the anabatic wind speed increases due to greater sensible heat fluxes even though drag on the anabatic wind is also greater (Figure 6a).

The vertical distribution of dust can be influenced by several factors. Increased surface roughness leads to greater sensible heat fluxes (Figure 6b) and hence more vertical mixing through turbulence. It follows that increasing the surface roughness decreases the percentage of the total dust mass at low levels (Figures 7c and 7d), since more dust is transported upwards through turbulent mixing. A greater percentage of dust lofted by haboobs remains at low levels compared to dust lofted by anabatic winds (Figure 7c). This is probably a result of increased stability and suppressed vertical mixing inside haboobs compared to their surroundings.

Both the mean and the standard deviation of the wind speed increase with greater slope or roughness (Figures 7e and 7f). This suggests that, as anabatic winds become faster, they loft greater masses of dust due to both greater mean wind speeds and greater turbulence. Haboob dust lofting is not affected much by topographic slope or anabatic winds (Figures 7a and 7b). Note that Figure 5a considers only the meridional—or in this case upslope—component of the wind speed, whereas Figures 7e and 7f consider both the zonal and the meridional component. The threshold velocity for dust lofting is small in these simulations due to the lack of vegetation and soil moisture. With a greater threshold velocity, anabatic winds may not be fast enough to loft dust.

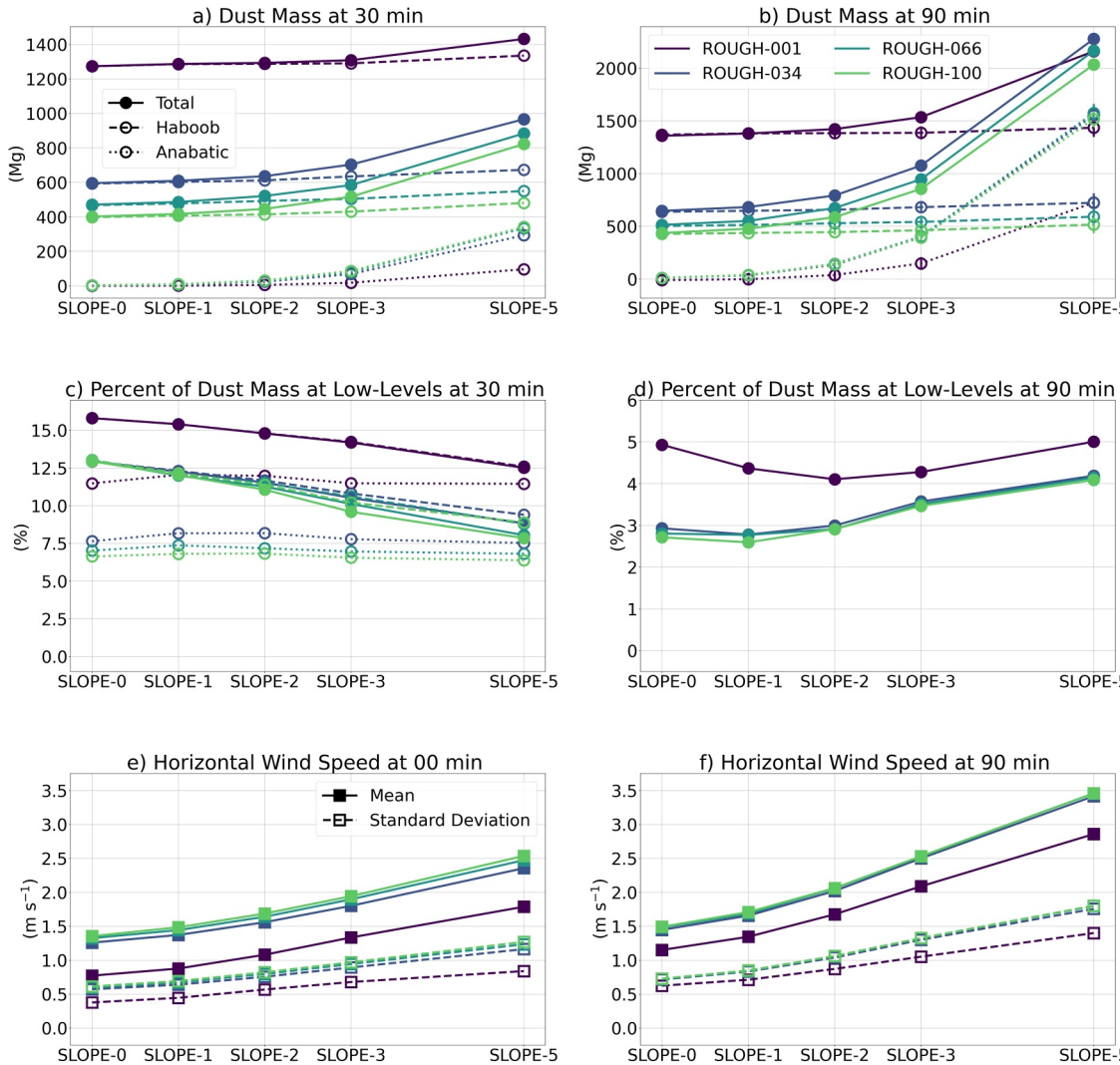

Figure 7. Increasing topographic slope increases the amount of lofted dust mostly due to the increased anabatic wind speeds. (a) Total dust mass (solid circles and lines), dust mass lofted by haboobs (hollow circles and dashed lines), and dust mass lofted by anabatic winds (hollow circles and dotted lines) as a function of topographic slope for different surface roughness (line colors) at 30 min. (b) as in (a) but for 90 min and with error bars (see Text S3 in Supporting Information S1 for an explanation of dust mass partitioning and error at 90 min). Note the vertical scale differs between (a) and (b). (c) as in (a) but showing the percent of the total dust mass at low levels (0–50 m AGL). (d) as in (c) but for 90 min. (e) Mean (solid squares and lines) and standard deviation (hollow squares and lines) horizontal wind speed at 0 min. (f) as in (e) but for 90 min.

The overall results of the suite of sensitivity experiments are summarized in Figure 8, which shows percent changes in haboob propagation speeds and dust lofting from the SLOPE-0_ROUGH-001 simulation. Compared to flat ground with low surface roughness, downslope haboob propagation speeds are reduced by 38.3% and dust lofting is increased by 49.7% on extreme slopes with large surface roughnesses (Figures 8a and 8d). Upslope haboob propagation speeds are less sensitive to changes in surface roughness and topographic slope than downslope speeds (Figures 8a and 8b). Increased surface roughness reduces dust lofting except on extreme slopes (Figure 8d). Most changes in Figure 8 are statistically significant at the $p < 0.001$ level. However, the upslope propagation speeds show fewer significant changes than the downslope propagation speeds or dust masses.

4. Conclusions

Haboobs are a major contributor to dust emissions in many regions (Bergametti et al., 2017; Heinold et al., 2013; Marsham et al., 2013). Many factors are known to influence haboob propagation speeds and dust lofting, such as turbulent mixing, low-level static stability, or surface vegetation types (H18, BvdH21, BvdH22). Haboobs

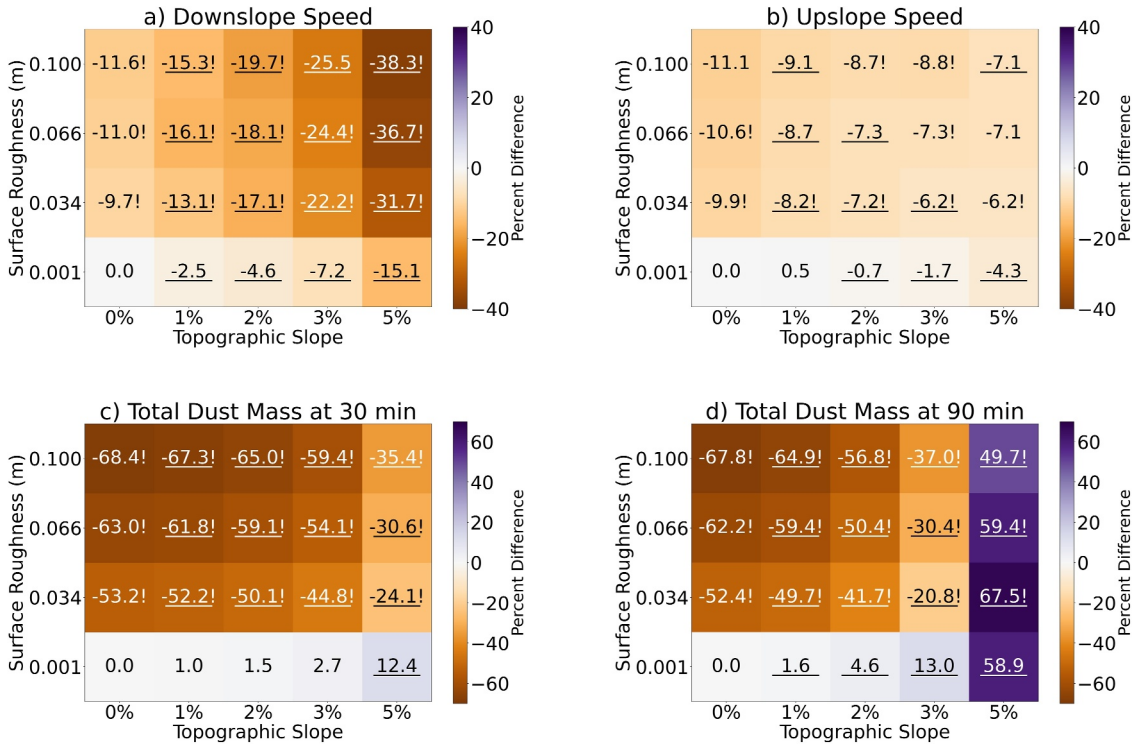

Figure 8. Summary of changes in propagation speeds and lofted dust mass with surface roughness and topographic slope. (a) Percent difference in mean downslope propagation speed from the SLOPE-0_ROUGH-001 simulation. (b) as in (a) but for upslope propagation speed. (c) Percent difference in total dust mass at 30 min. (d) as in (c) but at 90 min. Exclamation marks (underlines) indicate statistical significance from the simulation with the next smallest roughness (next smallest slope) at the $p < 0.001$ level. Note that, given this setup, the leftmost column of values cannot be underlined, and the bottom row of values cannot have exclamation marks.

commonly occur in regions of steeply sloped topography (Adams & Comrie, 1997; Knippertz et al., 2007; Miller et al., 2008), but the impact of topographic slope on haboobs—and cold pools more generally—has not been disentangled from these other known factors. Hence, the objective of this study has been to investigate the impacts of topographic slope on daytime haboob propagation and dust lofting, and how these impacts are modulated by surface roughness. Surface roughness was specifically tested as previous studies have demonstrated this factor can influence haboob propagation and dust lofting, but its influences are difficult to disentangle from those of other factors (e.g., vegetation type) (BvdH21, BvdH22). Haboobs in study are introduced at 1500 LT, making them representative of those formed by scattered afternoon convection and not by organized nocturnal convection. We used a suite of idealized high-resolution numerical experiments to achieve our objectives, the results of which are as follows and are shown schematically in Figure 9:

- On flat ground, increasing surface roughness decreases haboob propagation speeds and reduces the total mass of dust lofted by haboobs (Figures 8, 9e, and 9f).
- Without parameterized radiation or surface fluxes, haboobs propagate more rapidly downslope and less rapidly upslope compared to flat ground (Figure 5).
- With radiation and surface fluxes, as the topographic slope becomes steeper, the ground-relative downslope propagation speed of haboobs decreases, whereas the upslope propagation speed is mostly unchanged (Figures 8a, 8b, and 9).
- With radiation, an anabatic wind forms over sloped terrain, which becomes faster as the topographic slope becomes steeper and as the surface roughness increases (Figure 6a).
- Relative to the anabatic wind speed, the downslope propagation speed of haboobs is mostly unchanged and the upslope propagation speed decreases with increasing topographic slope (Figures 5b–5d).
- Thus, the anabatic wind speeds have a larger impact on the propagation speeds of haboobs than does the effect of the slope itself.
- As the topographic slope becomes steeper, dust lofting by the anabatic winds causes the total mass of dust lofted into the atmosphere to increase (Figures 8c, 8d, and 9).

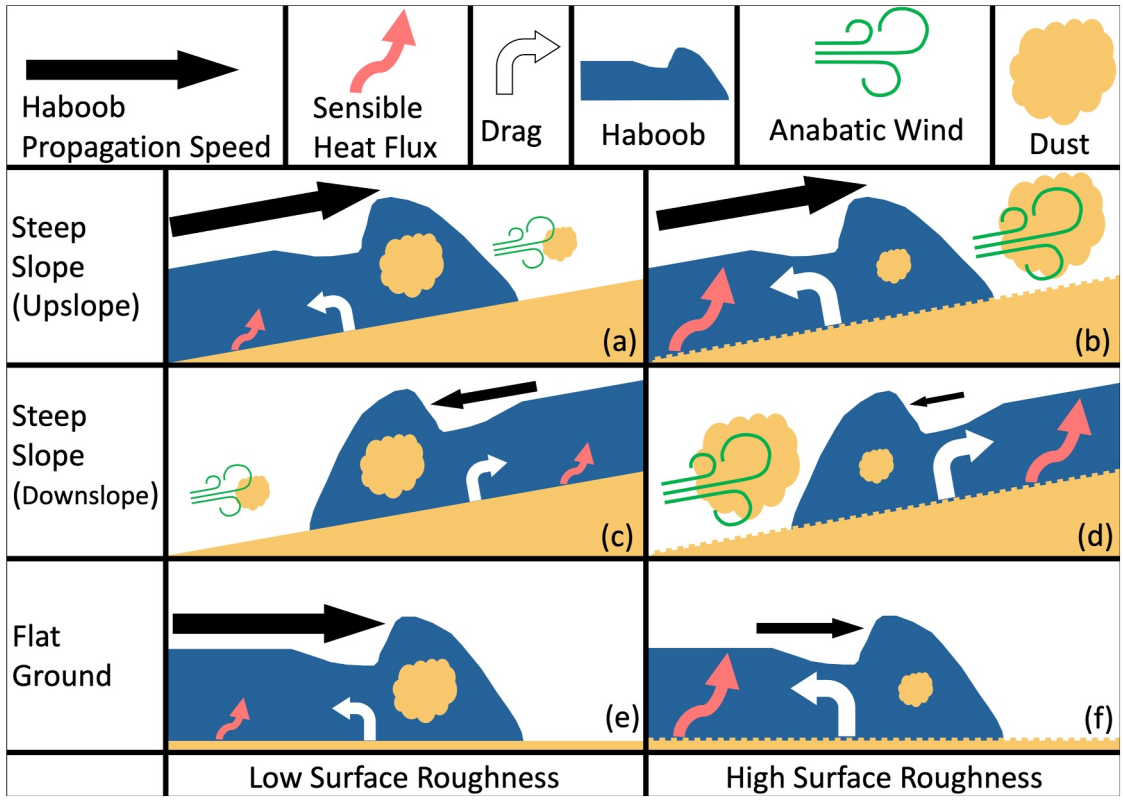

Figure 9. Schematic summary demonstrating the impacts of topographic slope and surface roughness. Larger objects are indicative of greater values, but the change in the size of objects between panels is not directly to scale. Dust clouds inside of haboobs are indicative of dust lofted by haboobs, whereas dust clouds outside of haboobs are indicative of dust lofted by anabatic winds.

The results of this study therefore suggest that the velocity of the anabatic winds that develop due to the heating of sloped terrain is of primary importance to the propagation and dust lofting of haboobs on such terrain.

The representation of complex topography and associated mesoscale processes is a large source of error in forecast models primarily around grid resolution. This study demonstrates that not only is the representation of haboob processes and anabatic winds in complex terrain important to properly representing dust lofting but so are the interactions between them. Climate model parameterization of cold pools (Pantillon et al., 2015; Rooney et al., 2022) should also consider ways in which to represent the impacts of such interactions to reduce errors in the amount of dust lofted by haboobs. We hope that the results of this study can be used to improve the representation of interactions between haboobs and anabatic winds in both small- and large-scale models. The results of this idealized study indicate that ambient wind speeds play a crucial role in determining cold pool propagation speeds in contrast to previous studies, which had found more mixed results (Luchetti, Friedrich, & Rodell, 2020; Luchetti, Friedrich, Rodell, et al., 2020). Finally, this study demonstrates that in haboob events occurring within mountainous regions that topographically driven winds not originating from haboobs or low-level jets may also be large contributors to dust emissions.

The findings of this study lead us to pose several new questions about haboob processes. What is the impact of topographic slope on haboobs at night? This study focused only on daytime conditions. Results at night may differ given the presence of katabatic winds as well as the nocturnal stratification of the boundary layer, which is known to affect haboobs (BvdH21). Also, what is the impact of complex terrain on haboobs? This study used linearly sloped terrain to ease the interpretation of results but results may vary with more complex terrain. Finally, what are the feedbacks between haboobs, topography, and storms? This study used dry conditions to facilitate the analysis, but the subsequent feedbacks to the parent storm producing the haboob are another avenue worth investigating. For example, previous studies have shown that cold pools in Northern Africa can sustain themselves for many hours by repeatedly initiating of new convective storms (Emmel et al., 2010; Knippertz

et al., 2007, 2009; Redl et al., 2015). These questions can best be addressed using a combination of idealized simulations, case-study simulations, and field work to leverage the distinct advantages of each of these approaches. As this study found a seemingly counterintuitive result—that haboobs propagate slower downslope than they propagate upslope in the presence of anabatic winds—investigating these questions may lead to further interesting physical insights on the relationships among haboobs, topography, land-atmosphere interactions, and convective storm processes.

Conflict of Interest

The authors declare no conflicts of interest relevant to this study.

Data Availability Statement

Model source code, name lists, and analysis scripts are available from Falk, Grant, and van den Heever (2025).

Acknowledgments
Funding was provided by NSF Grant AGS-2029611. We would like to acknowledge high-performance computing support from the Cheyenne and Derecho systems (https://doi.org/10.5065/qx9a-pg09) provided by the NSF National Center for Atmospheric Research (NCAR) sponsored by the National Science Foundation. We thank Bernd Heinold, two anonymous reviewers, and an associate editor for helpful comments which improved this study.

References

Adams, D. K., & Comrie, A. C. (1997). The North American monsoon. *Bulletin of the American Meteorological Society*, *78*(10), 2197–2213. https://doi.org/10.1175/1520-0477(1997)078<2197:tnam>2.0.co;2

Ansmann, A., Rittmeister, F., Engelmann, R., Basart, S., Jorba, O., Spyrou, C., et al. (2017). Profiling of Saharan dust from the Caribbean to western Africa -- Part 2: Shipborne lidar measurements versus forecasts. *Atmospheric Chemistry and Physics*, *17*(24), 14987–15006. https://doi.org/10.5194/acp-17-14987-2017

Ashley, W. S., Strader, S., Dziubla, D. C., & Haberlie, A. (2015). Driving blind: Weather-related vision hazards and fatal motor vehicle crashes. *Bulletin of the American Meteorological Society*, *96*(5), 755–778. https://doi.org/10.1175/bams-d-14-00026.1

Babin, S. M., Carton, J. A., Dickey, T. D., & Wiggert, J. D. (2004). Satellite evidence of hurricane-induced phytoplankton blooms in an oceanic desert. *Journal of Geophysical Research*, *109*(C3). https://doi.org/10.1029/2003JC001938

Benjamin, T. B. (1968). Gravity currents and related phenomena. *Journal of Fluid Mechanics*, *31*(2), 209–248. https://doi.org/10.1017/s0022112068000133

Bergametti, G., Marticorena, B., Rajot, J. L., Chatenet, B., Féron, A., Gaimoz, C., et al. (2017). Dust uplift potential in the central Sahel: An analysis based on 10 years of meteorological measurements at high temporal resolution. *Journal of Geophysical Research: Atmospheres*, *122*(22), 12433–12448. https://doi.org/10.1002/2017jd027471

Bristow, C. S., Hudson-Edwards, K. A., & Chappell, A. (2010). Fertilizing the Amazon and equatorial Atlantic with West African dust. *Geophysical Research Letters*, *37*(14). https://doi.org/10.1029/2010GL043486

Bryan, G. H., & Rotunno, R. (2014a). Gravity currents in confined channels with environmental shear. *Journal of the Atmospheric Sciences*, *71*(3), 1121–1142. https://doi.org/10.1175/jas-d-13-0157.1

Bryan, G. H., & Rotunno, R. (2014b). The optimal state for gravity currents in shear. *Journal of the Atmospheric Sciences*, *71*(1), 448–468. https://doi.org/10.1175/jas-d-13-0156.1

Bukowski, J., & van den Heever, S. C. (2020). Convective distribution of dust over the Arabian Peninsula: The impact of model resolution. *Atmospheric Chemistry and Physics*, *20*(5), 2967–2986. https://doi.org/10.5194/acp-20-2967-2020

Bukowski, J., & van den Heever, S. C. (2021). Direct radiative effects in haboobs. *Journal of Geophysical Research*, *126*(21), e2021JD034814. https://doi.org/10.1029/2021jd034814

Bukowski, J., & van den Heever, S. C. (2022). The impact of land surface properties on haboobs and dust lofting. *Journal of the Atmospheric Sciences*, *79*(12), 3195–3218. https://doi.org/10.1175/jas-d-22-0001.1

Caton Harrison, T., Washington, R., & Engelstaedter, S. (2021). Satellite-derived characteristics of Saharan cold pool outflows during boreal summer. *Journal of Geophysical Research*, *126*(3), e2020JD033387. https://doi.org/10.1029/2020jd033387

Cotton, W. R., Pielke, R. A., Sr., Walko, R. L., Liston, G. E., Tremback, C. J., Jiang, H., et al. (2003). RAMS 2001: Current status and future directions. *Meteorology and Atmospheric Physics*, *82*(1), 5–29. https://doi.org/10.1007/s00703-001-0584-9

Dai, A., & Huang, Y.-L. (2016). High-resolution simulations of non-Boussinesq downslope gravity currents in the acceleration phase. *Physics of Fluids*, *28*(2), 026602. https://doi.org/10.1063/1.4942239

Dai, A., Ozdemir, C. E., Cantero, M. I., & Balachandar, S. (2012). Gravity currents from instantaneous sources down a slope. *Journal of Hydraulic Engineering*, *138*(3), 237–246. https://doi.org/10.1061/(asce)hy.1943-7900.0000500

De Falco, M. C., Ottolenghi, L., & Adduce, C. (2020). Dynamics of gravity currents flowing up a slope and implications for entrainment. *Journal of Hydraulic Engineering*, *146*(4), 04020011. https://doi.org/10.1061/(asce)hy.1943-7900.0001709

Defant, F. (1951). Local winds. In T. F. Malone (Ed.), *Compendium of meteorology: Prepared under the direction of the committee on the compendium of meteorology* (pp. 655–672). American Meteorological Society.

DeMott, P. J., Sassen, K., Poellot, M. R., Baumgardner, D., Rogers, D. C., Brooks, S. D., et al. (2003). African dust aerosols as atmospheric ice nuclei. *Geophysical Research Letters*, *30*(14). https://doi.org/10.1029/2003GL017410

Dhital, S., Kaplan, M. L., Orza, J. A. G., & Fiedler, S. (2022). The Extreme North African Haboob in October 2008: High-resolution simulation of organized moist convection in the lee of the atlas, dust recirculation and poleward transport. *Journal of Geophysical Research: Atmospheres*, *127*(20), e2021JD035858. https://doi.org/10.1029/2021jd035858

Drager, A. J., Grant, L. D., & Heever, S. C. (2020). Cold pool responses to changes in soil moisture. *Journal of Advances in Modeling Earth Systems*, *12*(8), e2019MS001922. https://doi.org/10.1029/2019ms001922

Emmel, C., Knippertz, P., & Schulz, O. (2010). Climatology of convective density currents in the southern foothills of the Atlas Mountains. *Journal of Geophysical Research*, *115*(D11). https://doi.org/10.1029/2009JD012863

Falk, N. M., Grant, L. D., & van den Heever, S. C. (2025). Code and data associated with "Haboobs on Slopes" (Version v1) [Dataset]. *Zenodo*. https://doi.org/10.5281/zenodo.15126630

Falk, N. M., Grant, L. D., van den Heever, S. C., Ascher, B. D., Barbero, T. W., Davis, C. M., et al. (2025). Do cold pools propagate according to theory? *Journal of the Atmospheric Sciences*, *82*(8), 1481–1497. https://doi.org/10.1175/jas-d-24-0136.1

Farina, S., & Zardi, D. (2023). Understanding thermally driven slope winds: Recent advances and open questions. *Boundary-Layer Meteorology*, *189*(1), 5–52. https://doi.org/10.1007/s10546-023-00821-1

Field, P. R., Möhler, O., Connolly, P., Krämer, M., Cotton, R., Heymsfield, A. J., et al. (2006). Some ice nucleation characteristics of Asian and Saharan desert dust. *Atmospheric Chemistry and Physics*, *6*(10), 2991–3006. https://doi.org/10.5194/acp-6-2991-2006

Flamant, C., Chaboureau, J.-P., Parker, D. J., Taylor, C. M., Cammas, J.-P., Bock, O., et al. (2007). Airborne observations of the impact of a convective system on the planetary boundary layer thermodynamics and aerosol distribution in the inter-tropical discontinuity region of the West African Monsoon. *Quarterly Journal of the Royal Meteorological Society*, *133*(626), 1175–1189. https://doi.org/10.1002/qj.97

Gentine, P., Garelli, A., Park, S.-B., Nie, J., Torri, G., & Kuang, Z. (2016). Role of surface heat fluxes underneath cold pools. *Geophysical Research Letters*, *43*(2), 874–883. https://doi.org/10.1002/2015gl067262

Ginoux, P., Chin, M., Tegen, I., Prospero, J. M., Holben, B., Dubovik, O., & Lin, S.-J. (2001). Sources and distributions of dust aerosols simulated with the GOCART model. *Journal of Geophysical Research*, *106*(D17), 20255–20273. https://doi.org/10.1029/2000jd000053

Ginoux, P., Prospero, J. M., Gill, T. E., Hsu, N. C., & Zhao, M. (2012). Global-scale attribution of anthropogenic and natural dust sources and their emission rates based on MODIS Deep Blue aerosol products. *Reviews of Geophysics*, *50*(3). https://doi.org/10.1029/2012RG000388

Grant, L. D., & van den Heever, S. C. (2016). Cold pool dissipation. *Journal of Geophysical Research: Atmospheres*, *121*(3), 1138–1155. https://doi.org/10.1002/2015jd023813

Grant, L. D., & van den Heever, S. C. (2018). Cold pool-land surface interactions in a dry continental environment. *Journal of Advances in Modeling Earth Systems*, *10*(7), 1513–1526. https://doi.org/10.1029/2018ms001323

Griffin, D. W. (2007). Atmospheric movement of microorganisms in clouds of desert dust and implications for human health. *Clinical Microbiology Reviews*, *20*(3), 459–477. https://doi.org/10.1128/cmr.00039-06

Harrington, J. Y. (1997). *Effects of radiative and microphysical processes on simulated warm and transition season Arctic stratus*. Colorado State University.

He, Z., Zhao, L., Lin, T., Hu, P., Lv, Y., Ho, H.-C., & Lin, Y.-T. (2017). Hydrodynamics of gravity currents down a ramp in linearly stratified environments. *Journal of Hydraulic Engineering*, *143*(3), 04016085. https://doi.org/10.1061/(asce)hy.1943-7900.0001242

Heinold, B., Knippertz, P., Marsham, J. H., Fiedler, S., Dixon, N. S., Schepanski, K., et al. (2013). The role of deep convection and nocturnal low-level jets for dust emission in summertime West Africa: Estimates from convection-permitting simulations. *Journal of Geophysical Research D: Atmospheres*, *118*(10), 4385–4400. https://doi.org/10.1002/jgrd.50402

Hill, G. E. (1974). Factors controlling the size and spacing of cumulus clouds as revealed by numerical experiments. *Journal of the Atmospheric Sciences*, *31*(3), 646–673. https://doi.org/10.1175/1520-0469(1974)031<0646:fctsas>2.0.co;2

Houze, R. A., Jr. (2012). Orographic effects on precipitating clouds. *Reviews of Geophysics*, *50*(1). https://doi.org/10.1029/2011RG000365

Huang, Q., Marsham, J. H., Tian, W., Parker, D. J., & Garcia-Carreras, L. (2018). Large-eddy simulation of dust-uplift by a haboob density current. *Atmospheric Environment*, *179*, 31–39. https://doi.org/10.1016/j.atmosenv.2018.01.048

Johnson, R. H., Schumacher, R. S., Ruppert, J. H., Lindsey, D. T., Ruthford, J. E., & Kriederman, L. (2014). The role of convective outflow in the Waldo canyon fire. *Monthly Weather Review*, *142*(9), 3061–3080. https://doi.org/10.1175/mwr-d-13-00361.1

Kanatani, K. T., Ito, I., Al-Delaimy, W. K., Adachi, Y., Mathews, W. C., & Ramsdell, J. W. (2010). Desert dust exposure is associated with increased risk of asthma hospitalization in children. *American Journal of Respiratory and Critical Care Medicine*, *182*(12), 1475–1481. https://doi.org/10.1164/rccm.201002-0296oc

Kirshbaum, D. J. (2013). On thermally forced circulations over heated terrain. *Journal of the Atmospheric Sciences*, *70*(6), 1690–1709. https://doi.org/10.1175/jas-d-12-0199.1

Knippertz, P., Deutscher, C., Kandler, K., Müller, T., Schulz, O., & Schütz, L. (2007). Dust mobilization due to density currents in the Atlas region: Observations from the Saharan Mineral Dust Experiment 2006 field campaign. *Journal of Geophysical Research*, *112*(D21). https://doi.org/10.1029/2007JD008774

Knippertz, P., & Todd, M. C. (2012). Mineral dust aerosols over the Sahara: Meteorological controls on emission and transport and implications for modeling. *Reviews of Geophysics*, *50*(1). https://doi.org/10.1029/2011RG000362

Knippertz, P., Trentmann, J., & Seifert, A. (2009). High-resolution simulations of convective cold pools over the northwestern Sahara. *Journal of Geophysical Research*, *114*(D8). https://doi.org/10.1029/2008JD011271

Kok, J. F., Storelvmo, T., Karydis, V. A., Adebiyi, A. A., Mahowald, N. M., Evan, A. T., et al. (2023). Mineral dust aerosol impacts on global climate and climate change. *Nature Reviews Earth & Environment*, *4*(2), 71–86. https://doi.org/10.1038/s43017-022-00379-5

Lader, G., Raman, A., Davis, J. T., & Waters, K. (2016). Blowing dust and dust storms: One of Arizona's most underrated weather hazards. In *NOAA technical memorandum NWSWR-290*.

Li, J., Kandakji, T., Lee, J. A., Tatarko, J., Blackwell, J., Gill, T. E., & Collins, J. D. (2018). Blowing dust and highway safety in the southwestern United States: Characteristics of dust emission "hotspots" and management implications. *The Science of the Total Environment*, *621*, 1023–1032. https://doi.org/10.1016/j.scitotenv.2017.10.124

Lilly, D. K. (1962). On the numerical simulation of buoyant convection. *Tellus A Dynamic Meteorology and Oceanography*, *14*(2). https://doi.org/10.3402/tellusb.v14i2.13034

Liu, C., & Moncrieff, M. W. (2000). Simulated density currents in idealized stratified environments. *Monthly Weather Review*, *128*(5), 1420–1437. https://doi.org/10.1175/1520-0493(2000)128<1420:sdciis>2.0.co;2

Liu, H., Huang, Q., Chou, Y., Tian, H., Zhang, Y., Wu, X., et al. (2022). A numerical study of downbursts using the BLASIUS model. *Journal of Applied Meteorology and Climatology*, *61*(8), 1065–1076. https://doi.org/10.1175/jamc-d-21-0243.1

Lombardi, V., Adduce, C., Sciortino, G., & La Rocca, M. (2015). Gravity currents flowing upslope: Laboratory experiments and shallow-water simulations. *Physics of Fluids*, *27*(1), 016602. https://doi.org/10.1063/1.4905305

Luchetti, N. T., Friedrich, K., & Rodell, C. E. (2020). Evaluating thunderstorm gust fronts in New Mexico and Arizona. *Monthly Weather Review*, *148*(12), 4943–4956. https://doi.org/10.1175/mwr-d-20-0204.1

Luchetti, N. T., Friedrich, K., Rodell, C. E., & Lundquist, J. K. (2020). Characterizing thunderstorm gust fronts near complex terrain. *Monthly Weather Review*, *148*(8), 3267–3286. https://doi.org/10.1175/mwr-d-19-0316.1

Lugauer, M., Berresheim, H., Corsmeier, U., Dabas, A., Dyck, W., Emeis, S., et al. (2003). An overview of the VERTIKATOR project and results of Alpine pumping. In *Presented at the international conference alpine meteorology, Brig, CH*.

Mahowald, N. M., Kloster, S., Engelstaedter, S., Moore, J. K., Mukhopadhyay, S., McConnell, J. R., et al. (2010). Observed 20th century desert dust variability: Impact on climate and biogeochemistry. *Atmospheric Chemistry and Physics*, *10*(22), 10875–10893. https://doi.org/10.5194/acp-10-10875-2010

Marleau, L. J., Flynn, M. R., & Sutherland, B. R. (2014). Gravity currents propagating up a slope. *Physics of Fluids*, *26*(4), 046605. https://doi.org/10.1063/1.4872222

Marsham, J. H., Hobby, M., Allen, C. J. T., Banks, J. R., Bart, M., Brooks, B. J., et al. (2013). Meteorology and dust in the central Sahara: Observations from Fennec supersite-1 during the June 2011 intensive observation period. *Journal of Geophysical Research: Atmospheres*, *118*(10), 4069–4089. https://doi.org/10.1002/jgrd.50211

Martin, J. H., Gordon, R. M., & Fitzwater, S. E. (1990). Iron in Antarctic waters. *Nature*, *345*(6271), 156–158. https://doi.org/10.1038/345156a0

Meyer, B., & Haerter, J. O. (2020). Mechanical forcing of convection by cold pools: Collisions and energy scaling. *Journal of Advances in Modeling Earth Systems*, *12*(11), e2020MS002281. https://doi.org/10.1029/2020ms002281

Miller, S. D., Kuciauskas, A. P., Liu, M., Ji, Q., Reid, J. S., Breed, D. W., et al. (2008). Haboob dust storms of the southern Arabian Peninsula. *Journal of Geophysical Research*, *113*(D1). https://doi.org/10.1029/2007jd008550

Mulholland, J. P., Nesbitt, S. W., & Trapp, R. J. (2019). A case study of terrain influences on upscale convective growth of a supercell. *Monthly Weather Review*, *147*(12), 4305–4324. https://doi.org/10.1175/mwr-d-19-0099.1

Munson, S. M., Belnap, J., & Okin, G. S. (2011). Responses of wind erosion to climate-induced vegetation changes on the Colorado Plateau. *Proceedings of the National Academy of Sciences*, *108*(10), 3854–3859. https://doi.org/10.1073/pnas.1014947108

Neff, J. C., Ballantyne, A. P., Farmer, G. L., Mahowald, N. M., Conroy, J. L., Landry, C. C., et al. (2008). Increasing eolian dust deposition in the western United States linked to human activity. *Nature Geoscience*, *1*(3), 189–195. https://doi.org/10.1038/ngeo133

Pantillon, F., Knippertz, P., Marsham, J. H., & Birch, C. E. (2015). A parameterization of convective dust storms for models with mass-flux convection schemes. *Journal of the Atmospheric Sciences*, *72*(6), 2545–2561. https://doi.org/10.1175/jas-d-14-0341.1

Pantillon, F., Knippertz, P., Marsham, J. H., Panitz, H.-J., & Bischoff-Gauss, I. (2016). Modeling haboob dust storms in large-scale weather and climate models. *Journal of Geophysical Research: Atmospheres*, *121*(5), 2090–2109. https://doi.org/10.1002/2015jd024349

Pielke, R. A., Cotton, W. R., Walko, R. L., Tremback, C. J., Lyons, W. A., Grasso, L. D., et al. (1992). A comprehensive meteorological modeling system—RAMS. *Meteorology and Atmospheric Physics*, *49*(1), 69–91. https://doi.org/10.1007/bf01025401

Pokharel, A. K., Kaplan, M. L., & Fiedler, S. (2017). Subtropical dust storms and downslope wind events. *Journal of Geophysical Research: Atmospheres*, *122*(19), 10191–10205. https://doi.org/10.1002/2017jd026942

Prospero, J. M., Ginoux, P., Torres, O., Nicholson, S. E., & Gill, T. E. (2002). Environmental characterization of global sources of atmospheric soil dust identified with the nimbus 7 total ozone mapping spectrometer (TOMS) absorbing aerosol product. *Reviews of Geophysics*, *40*(1), 2-1–2-31. https://doi.org/10.1029/2000rg000095

Redl, R., Fink, A. H., & Knippertz, P. (2015). An objective detection method for convective cold pool events and its application to Northern Africa. *Monthly Weather Review*, *143*(12), 5055–5072. https://doi.org/10.1175/mwr-d-15-0223.1

Rooney, G. G., Stirling, A. J., Stratton, R. A., & Whitall, M. (2022). C-POOL: A scheme for modelling convective cold pools in the Met Office Unified Model. *Quarterly Journal of the Royal Meteorological Society*, *148*(743), 962–980. https://doi.org/10.1002/qj.4241

Saleeby, S. M., & van den Heever, S. C. (2013). Developments in the CSU-RAMS aerosol model: Emissions, nucleation, regeneration, deposition, and radiation. *Journal of Applied Meteorology and Climatology*, *52*(12), 2601–2622. https://doi.org/10.1175/jamc-d-12-0312.1

Saleeby, S. M., van den Heever, S. C., Bukowski, J., Walker, A. L., Solbrig, J. E., Atwood, S. A., et al. (2019). The influence of simulated surface dust lofting and atmospheric loading on radiative forcing. *Atmospheric Chemistry and Physics*, *19*(15), 10279–10301. https://doi.org/10.5194/acp-19-10279-2019

Seigel, R. B., & van den Heever, S. C. (2012a). Dust lofting and ingestion by supercell storms. *Journal of the Atmospheric Sciences*, *69*(5), 1453–1473. https://doi.org/10.1175/jas-d-11-0222.1

Seigel, R. B., & van den Heever, S. C. (2012b). Simulated density currents beneath embedded stratified layers. *Journal of the Atmospheric Sciences*, *69*(7), 2192–2200. https://doi.org/10.1175/jas-d-11-0255.1

Seigel, R. B., van den Heever, S. C., & Saleeby, S. M. (2013). Mineral dust indirect effects and cloud radiative feedbacks of a simulated idealized nocturnal squall line. *Atmospheric Chemistry and Physics*, *13*(8), 4467–4485. https://doi.org/10.5194/acp-13-4467-2013

Simpson, J. E. (1997). *Gravity currents*. Cambridge University Press.

Slingo, A., Ackerman, T. P., Allan, R. P., Kassianov, E. I., McFarlane, S. A., Robinson, G. J., et al. (2006). Observations of the impact of a major Saharan dust storm on the atmospheric radiation balance. *Geophysical Research Letters*, *33*(24). https://doi.org/10.1029/2006GL027869

Smagorinsky, J. (1963). General circulation experiments with the primitive equations: I. The basic experiment. *Monthly Weather Review*, *91*(3), 99–164. https://doi.org/10.1175/1520-0493(1963)091<0099:gcewtp>2.3.co;2

Smith, M. A. (2007). *Evaluation of mesoscale simulations of dust sources, sinks and transport over the Middle East*. Colorado State University.

Sokolik, I. N., & Toon, O. B. (1996). Direct radiative forcing by anthropogenic airborne mineral aerosols. *Nature*, *381*(6584), 681–683. https://doi.org/10.1038/381681a0

Stokowski, D. (2005). *The addition of the direct radiative effect of atmospheric aerosols into the Regional Atmospheric Modeling System (RAMS)*. Colorado State University.

Straka, J. M., Wilhelmson, R. B., Wicker, L. J., Anderson, J. R., & Droegemeier, K. K. (1993). Numerical solutions of a non-linear density current: A benchmark solution and comparisons. *International Journal for Numerical Methods in Fluids*, *17*(1), 1–22. https://doi.org/10.1002/fld.1650170103

Sutton, L. J. (1925). Haboobs. *Quarterly Journal of the Royal Meteorological Society*, *51*(213), 25–30. https://doi.org/10.1002/qj.49705121305

Tanaka, T. Y., & Chiba, M. (2006). A numerical study of the contributions of dust source regions to the global dust budget. *Global and Planetary Change*, *52*(1), 88–104. https://doi.org/10.1016/j.gloplacha.2006.02.002

Tong, D. Q., Gill, T. E., Sprigg, W. A., Van Pelt, R. S., Baklanov, A. A., Barker, B. M., et al. (2023). Health and safety effects of airborne soil dust in the Americas and beyond. *Reviews of Geophysics*, *61*(2), e2021RG000763. https://doi.org/10.1029/2021rg000763

Twohy, C. H., Kreidenweis, S. M., Eidhammer, T., Browell, E. V., Heymsfield, A. J., Bansemer, A. R., et al. (2009). Saharan dust particles nucleate droplets in eastern Atlantic clouds. *Geophysical Research Letters*, *36*(1). https://doi.org/10.1029/2008GL035846

van den Heever, S. C., Saleeby, S. M., Grant, L. D., Igel, A. L., & Freeman, S. W. (2022). *RAMS - The Regional Atmospheric Modeling System (Version v6.3.02)*. Zenodo. https://doi.org/10.5281/zenodo.6869798

Walker, A. L., Liu, M., Miller, S. D., Richardson, K. A., & Westphal, D. L. (2009). Development of a dust source database for mesoscale forecasting in southwest Asia. *Journal of Geophysical Research*, *114*(D18). https://doi.org/10.1029/2008JD011541

Walko, R. L., Band, L. E., Baron, J., Kittel, T. G. F., Lammers, R., Lee, T. J., et al. (2000). Coupled atmosphere–biophysics–hydrology models for environmental modeling. *Journal of Applied Meteorology and Climatology*, *39*(6), 931–944. https://doi.org/10.1175/1520-0450(2000)039<0931:cabhmf>2.0.co;2

Wu, C., Lin, Z., & Liu, X. (2020). The global dust cycle and uncertainty in CMIP5 (Coupled Model Intercomparison Project phase 5) models. *Atmospheric Chemistry and Physics*, *20*(17), 10401–10425. https://doi.org/10.5194/acp-20-10401-2020

References From the Supporting Information

Byers, H. R., & Braham, R. R. (1949). *The thunderstorm: Report of the thunderstorm project*. U.S. Government Printing Office.

Drager, A. J., & van den Heever, S. C. (2017). Characterizing convective cold pools. *Journal of Advances in Modeling Earth Systems*, *9*(2), 1091–1115. https://doi.org/10.1002/2016ms000788

van den Heever, S. C., Grant, L. D., Freeman, S. W., Marinescu, P. J., Barnum, J., Bukowski, J., et al. (2021). The Colorado State University Convective CLoud outflows and UpDrafts experiment (C3LOUD-Ex). *Bulletin of the American Meteorological Society*. https://doi.org/10.1175/bams-d-19-0013.1

Wills, S. M., Cronin, M. F., & Zhang, D. (2023). Air-sea heat fluxes associated with convective cold pools. *Journal of Geophysical Research: Atmospheres*, *128*(20), e2023JD039708. https://doi.org/10.1029/2023jd039708